ChemComm

Accepted Manuscript

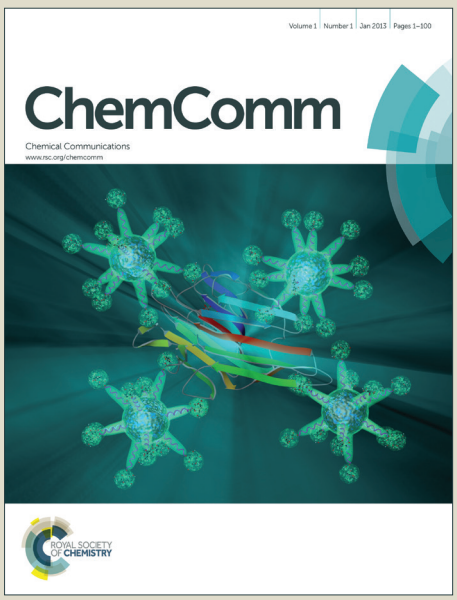

ROYAL SOCIETY OF CHEMISTRY

www.rsc.org/chemcomm

Cite this: DOI: 10.1039/c0xx00000x

www.rsc.org/chemcomm

COMMUNICATION

Unique electrocatalytic activity of nucleic acid-mimicking coordination polymer for sensitive detection of coenzyme A and histone acetyltransferase activity

Yufang Hu, Siyu Chen, Yitao Han, Hongjun Chen, Qin Wang, Zhou Nie,* Yan Huang, Shouzhuo Yao

Received (in XXX, XXX) Xth XXXXXXXXX 20XX, Accepted Xth XXXXXXXXX 20XX
DOI: 10.1039/b000000x

A nucleic acid-mimicking CoA-Ag(I) coordination polymer (CP) was *in-situ* prepared and its unique electrocatalytic activity to H_2O_2 reduction was discovered. Based on it, a novel, label-free electrochemical sensor has been developed for the sensitive detection of coenzyme A (CoA) and histone acetyltransferase (HAT) activity.

Organic-inorganic hybrid materials are unique materials that integrate functional organic components and inorganic building blocks via various chemical or physical interactions.[1] These materials are not the simple sum of two components but their synergic combination, hence the new composite material has distinct properties that were not observed in the individual components. Metal-organic ligand coordination polymers (CPs) are a typical subclass of these hybrid materials, whose structure, surface chemistry, and functionalities can be tuned or tailored from the atomic or molecular scale to the nanoscale through incorporation of different functional organic ligands and metal ions.[2] The applications of metal-organic CPs have penetrated in various fields, including catalysis, molecular recognition, sensing, biology, *etc*.[3] The further development of CP's applications is highly dependent on the discovery of new structures and functionalities of CPs via introducing new organic ligands.

Recent developments in the coordination polymers (CP) of coinage metal (Au, Ag, and Cu) and thiol compound have received great attention because of its unique physical properties and versatile applications, in which thiol-Ag(I) CP is a typical representative. The thiol-Ag(I) CP is formed by the reaction of thiols of organic molecule with Ag(I), yielding polymeric one-dimensional supermolecular structure with -thiol-Ag(I)- repeated segments, which is stabilized by thiol-Ag(I) interaction and aurophilic Ag(I)···Ag(I) interaction.[4] Because of its interesting chain-like structure with various functional groups, thiol-Ag(I) CP shows some unique properties, especially the optical properties of thiol-Ag(I) CP, which have been thoroughly studied and further successfully exploited in bio-detection of metal ion, small molecule, and enzyme activity.[5] However, to the best of our knowledge, the electrocatalytic activity of thiol-Ag(I) CP was seldom reported and its electrochemical biosensing application remains largely unexplored.

Coenzyme A (CoA) is an important coenzyme which functions in the activation and transfer of acyl groups.[6] It is a thiol compound composed by cysteine, pantothenate, and adenosine groups.[6] CoA and its acetylated form acetyl-coenzyme A (Ac-CoA) play key roles in central metabolism. Moreover, Ac-CoA/CoA pair is implicated in histone acetyltransferase (HAT)-catalyzed protein acetylation process, which is significant for the epigenetic regulation of gene expression.[7] Sensitive and selective bio-detection of CoA is highly demanded but most of available CoA biosensors rely on thiol-responsive probes, which are less specific.

Herein, we utilize CoA as organic ligand to prepare a novel nucleic-acid mimicking CoA-silver ion coordination polymer (CoA-Ag(I) CP) by a simple *in-situ* synthetic strategy. An unexpected high electrocatalytic activity of the prepared CoA-Ag(I) CP to H_2O_2 reduction was discovered and investigated. Furthermore, we have used this unique CoA-Ag(I) CP as electrochemical signal probe for highly sensitive and selective detection of coenzyme A. The detection mechanism relied on three intriguing phenomena that we found (Scheme 1): (1) Since two ends of CoA molecule are free thiol group and adenine respectively, the potential coordination polymer formed by CoA and Ag(I) was supposed as the chain-like structure with (-CoA-Ag(I)-) repeated units and multiple adenine bases as the side groups along the polymer backbone. So if CoA-Ag(I) CP is compared with nucleic acid, they both have multiple base side groups but CoA-Ag(I) CP possesses the thiol-Ag(I) CP backbone instead of the original pentose sugar/phosphate backbone of nucleic acid. Thus, in a way, CoA-Ag(I) CP is structurally similar to poly A single-stranded nucleic acid (ssNA), and it is named nucleic acid-mimicking CP hear (Scheme 1A); (2) inspired by the strong and selective interaction of ssNA with two-dimensional carbon nanomaterials, such as GO,[8] we discovered that CoA-Ag(I) CP, similar to ssNA, can easily and effectively bind with GO through its adenine side groups-caused π-π stacking interaction; (3) we further demonstrated that CoA-Ag(I) CP adsorbed on GO-modified electrode possesses high electrocatalytic activity to H_2O_2 reduction. Moreover, since CoA is the co-product of HAT-catalyzed protein acetylation, the proposed method was further adapted to quantitatively detect HAT activity via electrochemical measurement of CoA generation (Scheme 1B).

Characterization experiments have been done to verify the formation of CoA-Ag(I) CP, involving UV-vis spectroscopy, FT-IR spectra, and DLS experiments. As shown in Figure 1A, the absorbance peak at about 330 nm appears after mixing CoA and Ag(I), which is tentatively assigned to argentophilic interaction with the ligand-to-metal charge transfer transition and similar to those of other thiol-Ag(I) CPs,[4, 5] implying the formation of CoA-Ag(I) CP with -S-Ag(I)- repeated units. FT-IR spectra (Figure S1) further support the formation of S-Ag(I) bonds by the absence of stretching band of S-H of free CoA at 2555 cm^{-1}. In addition, dynamic light scattering (DLS) data show that the average

hydrodynamic diameter significantly increases to *ca.* 125±12 nm after the reaction of CoA and Ag(I) (Figure 1B), which is similar to that of the previously reported thiol-Ag(I) CP.[5b]

In order to test its nucleic acid-mimicking property, we further explored whether CoA-Ag(I) CP is capable of fluorescence enhancement of SYBR green II (SGII), a RNA-specific dye, considering its multiple adenine side groups. Interestingly, as we expect, the proposed CP stained by SGII exhibits strong fluorescence (Figure S2), which is 32.34-fold higher than that of SGII-only control. Meanwhile, the fluorescence intensity of SGII-stained CoA-Ag(I) CP (100 μM) is comparable to that of 2 μM 20 nt poly-A RNA stained by SGII (Figure S3), indicating the similarity between CoA-Ag(I) CP and RNA. Again, we used non-denaturing gel electrophoresis to further characterize CoA-Ag(I) CP. A bright smear band with quite large molecular weight is observed in CoA-Ag(I) CP sample (Figure S4), revealing that the running CoA-Ag(I) CP in the gel can also be stained by SGII, which is in agreement with that of fluorescence studies above.

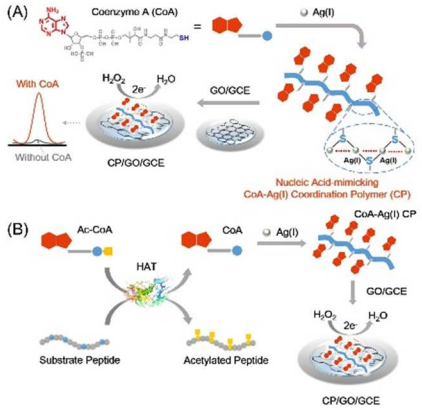

Scheme 1 Schematic diagrams of (A) the synthesis of nucleic acid-mimicking CoA-Ag(I) CP and its electrocatalytic activity on GO-modified electrode and (B) the electrochemical biosensor for probing HAT activity based on GO and CoA-Ag(I) CP.

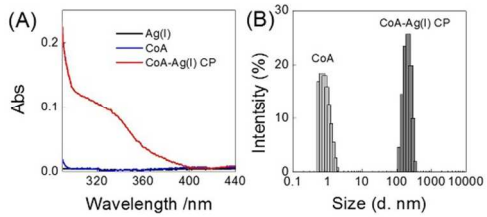

Fig. 1 (A) UV-vis absorption spectra of CoA-Ag(I) CP in 0.1 M HAc-NaAc (pH 5.0); (B) Size distributions of CoA-Ag(I) CP determined by dynamic light scattering (DLS). [CoA] = [Ag(I)] = 100 μM.

Hence we expected that CoA-Ag(I) CP, similar to RNA, could interact with GO with high affinity. To explore the binding of CoA-Ag(I) CP and GO, the mixture of GO and CoA-Ag(I) CP was centrifuged, then the supernatant was taken out and used for the fluorescence measurement and the precipitate was characterized by fourier transform infrared spectrometry (FT-IR) and atomic force microscopy (AFM) experiments. As noted in Figure S5, CoA-Ag(I) CP without GO shows no change for fluorescence signal after centrifugation, indicating that almost all of CoA-Ag(I) CP stays in supernatant. Oppositely, there is a sharp fluorescence decrease at 530 nm for the supernatant of the mixture of CoA-Ag(I) CP and GO after centrifugation, suggesting that CoA-Ag(I) CP is firmly attached on GO surface and becomes the precipitant together with GO. The FI-IR spectra of the resulting precipitant (Figure S6) show not only the stretching band of GO but also some characteristic stretching bands of CoA-Ag(I) CP, for example, the peaks at 1255 cm^{-1} and 1090 cm^{-1} which are assigned to stretching vibration of P=O and P-O of CoA, respectively, indicating the binding of CoA-Ag(I) CP on GO. AFM was also employed to characterize the binding interaction of GO and CoA-Ag(I) CP. As shown in Figure 2A, a thin layer of GO with approximately 1 nm was observed on mica substrate. However, when GO was incubated with CoA or $AgNO_3$ (Figure 2B, C), we cannot observe any discrepancy in AFM images and the associated height profiles. When CoA-Ag(I) CP were used, a number of long chain-like substances with different lengths can be observed on GO surface (Figure 2D and S7). The associated height profiles display that the average height of CoA-Ag(I) CP is about 2 nm (Figure 2D). Moreover, with the increase of the concentrations of CoA-Ag(I) CP from 100 μM to 2 mM, more chain-like structures can be found in AFM images (Figure S8). These results directly confirm that self-assembly of CoA and Ag(I) can create long chain-like CoA-Ag(I) CP nanostructures, which can be adsorbed firmly onto the GO surface.

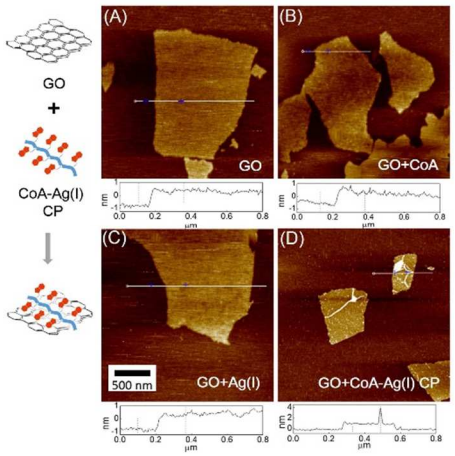

Fig. 2 Atomic force microscopy (AFM) images of (A) GO, (B) GO and CoA, (C) GO and Ag(I), and (D) GO and CoA-Ag(I) CP for demonstrating affinity interaction of CoA-Ag(I) CP and GO. Line charts in the bottom of these AFM images are associated height profiles.

Afterwards, we verified the adsorption of CoA-Ag(I) CP on GO by electrochemical measurements. As illustrated in Figure S9A, the cyclic voltammetry (CV) signal of $[Fe(CN)_6]^{3-/4-}$ sharply decreases (red) in response to the adsorption of CoA-Ag(I) CP on the surface of GO-modified glassy carbon electrode (GO/GCE) because of the electrostatic repulsion between anionic $[Fe(CN)_6]^{3-/4-}$ and negatively charged CP (deriving from phosphate group of CoA). Subsequently, electrochemical impedance spectroscopy (EIS) was employed to further monitor the modified electrodes and a sharp increase of electron transfer resistance (R_{et}) at CoA-Ag(I) CP-treated electrode (CP/GO/GCE) was indicative of the adsorption of CoA-Ag(I) CP on GO (Figure S9B).

It was intriguing that we discovered the electrocatalytic property of CoA-Ag(I) CP, which is largely unexplored. To assess it, a series of electrochemical measurements of CV were carried out in the presence of H_2O_2. As shown in Figure 3A, both the bare GCE and GO/GCE show no redox peaks, while an outstanding reduction peak is observed near -0.7 V at CP/GO/GCE, which indicates the electrochemical reduction of H_2O_2. The absence of any of the reactants (CoA or Ag(I) alone) also leads to negligible electrochemical signal (Figure 3A). It is evident that the high electrocatalytic activity could be ascribed to CoA-Ag(I) CP. We have tried to directly deposit the CoA-Ag(I) CP on bare electrode (CP/GCE), and no obvious electrocatalytic

activity to H_2O_2 reduction was observed (Figure 3B), implying that GO is also important for loading CoA-Ag(I) CP and supporting it to achieve efficient electrocatalytic activity.

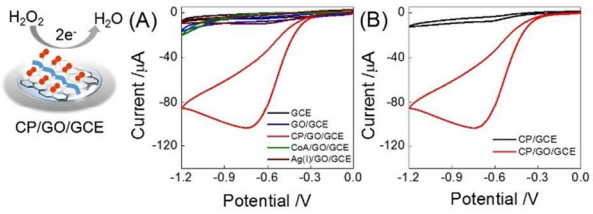

Fig. 3 (A) Cyclic voltammograms of bare GCE, GO-electrodeposited GCE (GO/GCE), CoA-Ag(I) CP-adsorbed GO/GCE (CP/GO/GCE), CoA-adsorbed GO/GCE (CoA/GO/GCE) and Ag(I)-adsorbed GO/GCE (Ag(I)/GO/GCE) and (B) Cyclic voltammograms of CP/GO/GCE and CoA-Ag(I) CP-adsorbed GCE (CP/GCE) in N_2-saturated 100 mM PBS (pH 7.0) with 5 mM H_2O_2. [CoA] = [Ag(I)] =100 μM.

To investigate the electrocatalytic mechanism of CoA-Ag(I) CP, CVs were performed to probe the redox reactions of Ag species at CP/GO/GCE in the absence of H_2O_2. As shown in Figure S10, during the 1st cycle of CV scanning from -0.1 V to +0.4 V, CP/GO/GCE shows negligible oxidation peak of Ag(0) and a distinct reduction peak of Ag(I) near 0 V, indicating the dominant silver species in original CoA-Ag(I) CP is Ag(I). Then, CP/GO/GCE was pre-treated by CV scanning from -1.2 V to 0 V for 10 cycles, which mimics the CV condition of electrocatalytic study. The pre-treated CP/GO/GCE was subsequently examined by CV scanning from -0.1 V to +0.4 V, an outstanding oxidation peak of Ag(0) at +0.224 V, indicative of the presence of Ag(0), is observed,[9] clearly evidencing the reduction of Ag(I) to Ag(0) of the coordination polymer. To further study whether the reduced Ag(0) accounts for the electrocatalytic reduction of H_2O_2, we prepared CoA-capped silver nanoclusters (CoA-AgNCs) as the control via reduction of CoA-Ag(I) CP by $NaBH_4$. Figure S11 shows that upon $NaBH_4$ reduction the original absorption of CoA-Ag(I) CP at 330 nm disappears but a new band near 450 nm appears, which is indicative of AgNCs.[10] Moreover, the resulting AgNCs showed strong fluorescence emission at 540 nm (excitation at 470 nm, Figure S12). Figure S13 illustrates that both CoA-Ag(I) CP-loaded electrode (CP/GO/GCE) and CoA-AgNCs-loaded electrode (AgNCs/GO/GCE) can efficiently catalyze the electrochemical reduction of H_2O_2, and CP/GO/GCE displays better electrocatalytic performance relative to AgNCs/GO/GCE. Moreover, we also found that the direct electrodeposition of Ag(0) on GO/GCE electrode (Ag(0)/GO/GCE) also possesses effective electrocatalytic activity to H_2O_2 reduction (Figure S14). Consequently, we elucidated that CoA-Ag(I) CP-induced electrocatalytic reduction might result from the resulting CoA-Ag(0) CP or tiny AgNCs in the electrochemical scanning process. By referring to the literature,[11] the plausible mechanism could be deduced as follows:

$$\text{CoA-Ag(I) CP} + e^- \longrightarrow \text{CoA-Ag(0) CP at the electrode} \quad (1)$$

$$2\ \text{CoA-Ag(0) CP} + H_2O_2 \longrightarrow 2\text{CoA-[Ag(I)-OH] CP} \quad (2)$$

$$2\ \text{CoA-[Ag(I)-OH] CP} + 2e^- + 2H^+ \longrightarrow 2\text{CoA-Ag(0) CP} + H_2O \quad (3)$$

Some experimental parameters influential in electrocatalytic activity of CP/GO/GCE have been optimized (Figure S15). The best optimal values for the electrodeposition cycles of GO on GCE, adsorption time of CoA-Ag(I) CP on GO/GCE, and pH of supporting electrolyte were found to be 10 cycles, 10 min, and pH 7.0, respectively.

Based on the unique electrocatalytic activity of CoA-Ag(I) CP, a novel electrochemical sensor has been developed for quantitative detection of CoA. Under the above-mentioned optimized conditions, we assessed the effect of CoA concentration on electrochemical signal upon fixing Ag(I) concentration (100 μM). As shown in Figure 4A, increasing response currents are observed with the increment of CoA concentration from 0 to 100 μM. Then, a linear relationship (Figure 4B) is obtained between increasing current response and CoA concentrations ranging from 0.1 μM to 100 μM, and the detection limit is 0.05 μM (S/N=3).

Since both thiol and adenine group of CoA are essential for the synthesis of unique nucleic acid-mimicking CP, we examined the response of the proposed sensor to some of thiol-containing or adenine-containing compounds in order to test the specificity of the sensor to CoA. As illustrated in Figure 4C, thiol-containing compounds, including glutathione (GSH), *L*-cysteine (*L*-Cys) and tripeptide (GCG), display no obvious electrochemical signal owing to lack of the side groups which can strongly bind with GO via π-π stacking. Some adenine-containing ligands, such as adenine, adenosine triphosphate (ATP) and adenosine monophosphate (AMP), are subsequently evaluated (Figure 4C), and negligible electrochemical signals were observed, indicating that these compounds are incapable to form CP with Ag(I). Consequently, the proposed sensor exhibits high specificity to CoA.

Furthermore, the storage stability of the biosensor was investigated by monitoring its response to 5 mM H_2O_2 (Figure S16). After a month, the proposed sensor remains stable and the response current is approximately 83.7% of the original current. To testify the potential application of our method in real biological systems, a CoA-trapping test was performed in human serum samples spiked with different concentrations of CoA. The recoveries are between 96.7% and 108.5% (Table S1), providing a new insight into CoA-relevant determination in biological fluids such as serum.

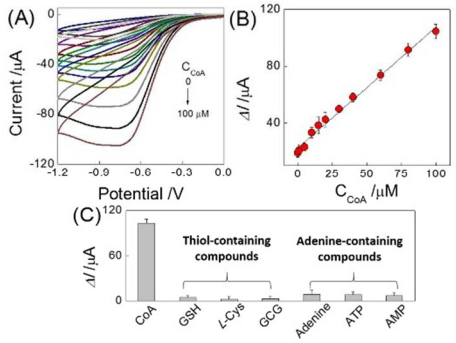

Fig. 4 (A) Cyclic voltammograms of CP/GO/GCE in N_2-saturated 100 mM PBS (pH 7.0) in the presence of H_2O_2 (5 mM) with different CoA concentrations (from top to bottom: 0, 0.1, 1, 5, 10, 15, 20, 30, 40, 60, 80, and 100 μM) and the fixed $AgNO_3$ concentration (100 μM); (B) Plot of electrocatalytic reduction peak current of H_2O_2 *versus* CoA concentrations; (C) The electrochemical signals of the proposed sensor in response to CoA, other thiol-containing ligands (glutathione (GSH), *L*-cysteine (*L*-Cys), and the tripeptide (GCG)), and other adenine-containing ligands (adenine, adenosine triphosphate (ATP), and adenosine monophosphate (AMP)), the concentration of all ligands was 100 μM, [Ag(I)] = 100 μM.

The proposed CoA-Ag(I) CP and its electrocatalytic activity were further employed for probing the enzymatic activity of HAT (Scheme 1B). The transcriptional activator protein p300 is used as model HAT enzyme in our work. HAT p300 catalyzes the transfer of an acetyl group from Ac-CoA to lysine residue of substrate peptide, producing ε-N-acetyl lysine residue and CoA, so that HAT activity can be facilely probed by monitoring CoA generation. Figure S17 shows that the whole HAT reaction mixture induces remarkable current response, while the absence of any of the reactants leads to no obvious electrochemical signal,

indicating the feasibility of the proposed sensor for HAT activity detection. The quantitative detection of HAT activity was carried out with different concentrations of p300 (Figure 5A). The corresponding calibration curve is shown in Figure 5B, the linear range is from 0.1 to 100 nM with the detection limit of 0.067 nM (S/N=3), which is lower than those of most of previously-reported HAT assays (Table S2). Furthermore, the selectivity of the HAT sensor was evaluated by challenging the sensor with various proteins (Figure S18) and was displayed an excellent selectivity.

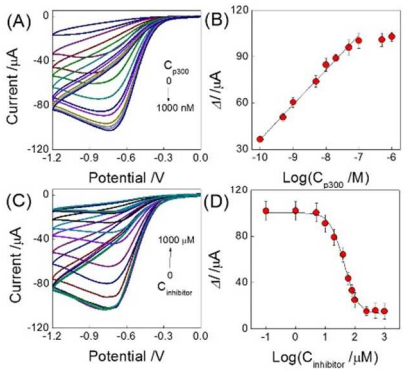

Fig. 5 Detection of HAT by electrochemical assay at the CP/GO/GCE in N_2-saturated 100 mM PBS (pH 7.0) with 5 mM H_2O_2: (A) Cyclic voltammograms in response to different concentrations of p300 HAT (From top to bottom: 0, 0.1, 0.5, 1.0, 5.0, 10, 20, 50, 100, 500, and 1000 nM); (B) Calibration curve of the proposed HAT sensor. Detection of HAT inhibition by the electrochemical assay at the CP/GO/GCE in N_2-saturated 100 mM PBS (pH 7.0) with 5 mM H_2O_2, the concentration of p300 was 100 nM: (C) Various concentrations of anacardic acid were used for investigation of HAT inhibition. From bottom to top: 0, 0.1, 1.0, 5.0, 10, 20, 40, 60, 80, 100, 250, 500, and 1000 μM; (D) Electrochemical signal as a function of the concentration of anacradic acid.

To test whether the electrochemical HAT assay can be employed to quantitatively assess HAT inhibitor, anacardic acid, a potent small molecule inhibitor of the HAT, is used for testing the feasibility of the proposed sensor in inhibitors screening.[12] As shown in Figure 5C, the electrochemical signal decreases gradually with increasing concentration of anacardic acid because of the inhibition of p300 activity and thus low level of peptide acetylation. Then the IC_{50} value (half maximal inhibitory concentration of the inhibitor) is determined to be 48.61±10 μM (Figure 5D), which is well consistent with the literature values,[13] suggesting a potential to qualitatively screen HAT inhibitors.

In summary, we discovered a unique electrocatalytic activity of CoA-Ag(I) CP, which facilitates us to develop a novel, simple, label-free, and sensitive electrochemical method to probe CoA and HAT activity. We demonstrated CoA and Ag(I) could yield a novel nucleic acid-mimicking coordination polymer because of its intriguing structure with thiol and adenine group; the formed CoA-Ag(I) CP, similar to RNA, has strong affinity with GO; the resulting CoA-Ag(I) CP-bound GO/GCE showed the remarkably enhanced electro-catalysis toward H_2O_2 reduction. The proposed sensor exhibits excellent specificity to CoA, which is hardly achieved by traditional methods. Moreover, this method further shows the feasibility to detect the enzymatic activity of a key epigenetic enzyme, HAT. To the best of our knowledge, this work exhibits the first example of electrochemical sensor for detection of HAT activity. After all, this work presents a new functionality of a novel biomimetic CP, proving the great potential of functional CPs in biosensing and biological research.

This work was financially supported by the National Natural Science Foundation of China (Nos. 21222507, 21175036, 21235002, and 21475038), the National Basic Research Program of China (973 Program, No. 2011CB911002), the Foundation for Innovative Research Groups of NSFC (Grant 21221003), and the Ph.D. Programs Foundation of the Ministry of Education of China (No.20120161110025).

Notes and references

State Key Laboratory of Chemo/Biosensing and Chemometrics, College of Chemistry and Chemical Engineering, Hunan University, Changsha, 410082, P. R. China.. Fax: +86-731-88821848; Tel: +86-731-88821626; E-mail: niezhou.hnu@gmail.com

† Electronic Supplementary Information (ESI) available: [details of any supplementary information available should be included here].

1 H. B. Yao, M. R. Gao and S. H. Yu, *Nanoscale*, 2010, **2**, 323-334.

2 (a) T. R. Cook, Y. R. Zheng and P. J. Stang, *Chem. Rev.*, 2013, **113**, 734-777; (b) W. L. Leong and J. J. Vittal, *Chem. Rev.*, 2011, **111**, 688-764.

3 (a) P. G. Bruce, B. Scrosati and J. M. Tarascon, *Angew. Chem. Int. Ed.*, 2008, **47**, 2930-2946; (b) D. W. Hatchett and M. Josowicz, *Chem. Rev.*, 2008, **108**, 746-769; (c) W. J. Chen, L.Y. Zheng, M. L. Wang, Y. W. Chi and G. N. Chen, *Anal. Chem.*, 2013, **85**, 9655-9663; (d) J. J. Deng, P. Yu, Y. X. Wang and L. Q. Mao, *Anal. Chem.*, 2015, **87**, 3080-3086.

4 (a) D. H. Li, J. S. Shen, N. Chen, Y. B. Ruan and Y. B. Jiang, *Chem. Commun.*, 2011, **47**, 5900-5902; (b) Q. Zhang, Y. Hong, N. Chen, D. D. Tao, Z. Li and Y. B. Jiang, *Chem. Commun.*, 2015, **51**, 8017-8019.

5 (a) J. S. Shen, D. H. Li, Q. G. Cai and Y. B. Jiang, *J. Mater. Chem.*, 2009, **19**, 6219-6224; (b) J. S. Shen, D. H. Li, M. B. Zhang, J. Zhou, H. Zhang and Y. B. Jiang, *Langmuir*, 2011, **27**, 481-486; (c) D. L. Liao, J. Chen, H. P. Zhou, Y. Wang, Y. X. Li and C. Yu, *Anal. Chem.*, 2013, **85**, 2667-2672.

6 (a) P. K. Mishra and D. G. Drueckhammer, *Chem. Rev.*, 2000, **100**, 3283-3309; (b) J. Baddiley, E. M. Thain, G. D. Novelli and F. Lipmann, *Nature*, 1953, **171**, 76.

7 (a) Y. Y. Yang and H. C. Hang, *ChemBioChem*, 2011, **12**, 314-322; (b) S. Y. Chen, Y. Li, Y. F. Hu, Y. T. Han, Y. Huang, Z. Nie and S. Z. Yao, *Chem. Commun.*, 2015, **51**, 4469-4472; (c) Y. T. Han, P. Li, Y. T. Xu, H. Li, Z. L. Song, Z. Nie, Z. Chen and S. Z. Yao, *Small*, 2015, **11**, 877-885.

8 (a) L. H. Tang, Y. Wang, Y. Liu and J. H. Li, *ACS Nano*, 2011, **5**, 3817-3822; (b) L. Lin, Y. Liu, X. Zhao and J. H. Li, *Anal. Chem.*, 2011, **83**, 8396-8402.

9 M. R. Guascito, E. Filippo, C. Malitesta, D. Manno, A. Serra and A. Turco, *Biosens. Bioelectron.*, 2008, **24**, 1057-1063.

10 J. T. Petty, J. Zheng, N. V. Hud and R. M. Dickson, *J. Am. Chem. Soc.*, 2004, **126**, 5207-5212.

11 (a) Y. L. Xia, W. H. Li, M. Wang, Z. Nie, C. Y. Deng and S. Z. Yao, *Talanta*, 2013, **107**, 55-60; (b) C. I. Richards, S. Choi, J. C. Hsiang, Y. Antoku, T. Vosch, A. Bongiorno, Y. L. Tzeng and R. M. Dickson, *J. Am. Chem. Soc.*, 2008, **130**, 5038-5039.

12 Y. Sun, X. Jiang, S. Chen and B. D. Price, *FEBS Lett.*, 2006, **580**, 4353-4356.

13 J. E. Ghadiali, S. B. Lowe and M. M. Stevens, *Angew. Chem. Int. Ed.*, 2011, **50**, 3417-3420.